

Wi-Fi Hotspot at Signalized Intersection: Cost-Effectiveness for Vehicular Internet Access

Ning Lu, *Student Member, IEEE*, Nan Cheng, *Student Member, IEEE*, Ning Zhang, *Student Member, IEEE*, Xuemin (Sherman) Shen, *Fellow, IEEE*, Jon W. Mark, *Life Fellow, IEEE*, Fan Bai, *Member, IEEE*

Abstract—In this paper, we investigate the cost-effectiveness of Wi-Fi solution for vehicular Internet access. We define the cost-effectiveness as the cost saving by deploying and operating a low-cost Wi-Fi infrastructure instead of a costly benchmark cellular network. To characterize the service quality of Wi-Fi deployment, we also define the normalized service delay which is the service time to fulfill a data application via the Wi-Fi network normalized by that via the cellular network. To derive the service time, we analyze the average throughput capacity of a generic vehicle in the Wi-Fi network and the average downlink capacity in the cellular network. Especially, we propose deploying Wi-Fi access point at signalized intersection and study the fundamental influence of traffic signals (which yield an interrupted vehicle traffic) on Wi-Fi access. Then, we examine the tradeoff between cost-effectiveness and normalized service delay by identifying interplays between controllable (e.g., the density of Wi-Fi deployment and user's satisfaction) and uncontrollable parameters (e.g., vehicle traffic statistics). Our results are very useful for network operators to make strategic planning of Wi-Fi deployment for vehicular Internet Access.

I. INTRODUCTION

With growing awareness of road safety and the ever-increasing demand for high-speed mobile Internet services, Internet connectivity is becoming a must-have feature of modern vehicles. The telecommunication industry has responded promptly by using off-the-shelf wireless technologies to establish a huge mass market of Internet-connected cars, which is expected to reach USD 131.9 billion by 2019 [1]. Not surprisingly, cellular technology, such as 3G (UMTS, HSPA, HSPA+) and 4G (LTE), is the top choice for delivering Internet service to cars due to its prominent role in providing reliable and ubiquitous mobile Internet access. Very recently, via AT&T's LTE network, General Motors's LTE-connected car has begun hitting the roads, powering many automotive telematics applications (e.g., emergency services and online diagnostics) [2]. However, the cellular network nowadays faces an uphill battle against the explosive growth of mobile data traffic which has been reportedly doubling each year in the last

few years. Exploiting complementary spectrum for vehicular Internet access is thereby an immediate need, which is also part of the solution to the so-called 1000x data challenge [3].

Operating in unlicensed frequency bands, Wi-Fi is astonishingly popular with millions of hotspots deployed all over the world for public Internet access. Due to its low per-bit cost and the feasibility of serving outdoor users at vehicular mobility [4], Wi-Fi is expected to be an attractive and complementary tool to deliver broadband services to moving cars — the built-in Wi-Fi radio or Wi-Fi-enabled mobile devices on board can access the Internet when vehicles *drive-thru* the coverage of Wi-Fi hotspots. Recent advances in Passpoint/Hotspot 2.0, powered by Wi-Fi Alliance, make Wi-Fi more capable of providing secure connectivity than before. Moreover, with subscriber identity module (SIM)-based authentication, seamless roaming between Wi-Fi and cellular networks is also enabled.

Compared to cellular access with wide availability, the Wi-Fi infrastructure has limited utility of the service offering for vehicles over intermittent network connectivity, as observed in real-world tests, e.g., [5]. Typically, vehicle users on the road have to experience a number of drive-thrus/connections to fulfill a mobile application (e.g., buffering a video clip of 100 MBytes from the Internet), implying a large service delay that degrades the user's satisfaction. While the Wi-Fi footprint can be enlarged by deploying more Wi-Fi access points (APs) [6], the network cost or TCO¹ would be increased as well. Especially, a solution that tries to achieve a ubiquitous coverage as cellular networks is prohibitive and not practical [7]. Therefore, great uncertainty remains as to whether it makes economic sense to deploy Wi-Fi networks for highly mobile vehicle users. Thanks to the new generation Wi-Fi hotspot, many mobile network operators (MNOs), such as AT&T and China Mobile, have shown strong interest in the Wi-Fi solution. However, the real benefit of Wi-Fi solution should be validated through cost-effectiveness analysis considering user's satisfaction so that MNOs would be fully convinced to turn the strong interest to strong commitment to deploy large-scale outdoor Wi-Fi networks in favor of vehicle users.

As an effort to that end, in this paper, we study cost-effectiveness of vehicular Internet access through Wi-Fi hotspots. The *cost-effectiveness* is defined as the TCO saving by deploying and operating drive-thru Wi-Fi networks instead of the cellular network for vehicular Internet access. To establish the relationship between cost-effectiveness and network

Copyright (c) 2015 IEEE. Personal use of this material is permitted. However, permission to use this material for any other purposes must be obtained from the IEEE by sending a request to pubs-permissions@ieee.org.

N. Lu, N. Cheng, N. Zhang, X. Shen, and J.W. Mark are with the Department of Electrical and Computer Engineering, University of Waterloo, 200 University Avenue West, Waterloo, Ontario, Canada N2L 3G1 (e-mail: {n7lu, n5cheng, n35zhang, sshen, jwmark}@uwaterloo.ca).

F. Bai is with General Motors Corporation, ECI Lab, Warren, MI 48092, USA (e-mail: fan.bai@gm.com).

This work is financially supported by a joint research grant from NSERC and General Motors.

¹Total cost of ownership, including one-time cost component (CAPEX, capital expenditures) and recurring cost component (OPEX, operational expenditures).

performance, we analyze the maximum average throughput of individual vehicle under any given density of deployed Wi-Fi APs (different deployment yields different cost-effectiveness), which can be used to determine the service delay once the total throughput required for fulfilling a data application is given. For apple-to-apple comparison, the network performance of benchmark cellular network is also analyzed so that the service delay experienced in Wi-Fi network can be normalized by that in cellular network. This *normalized service delay* is then able to reflect the service quality degradation because of using Wi-Fi networks characterized by the corresponding cost-effectiveness. We examine tradeoff between cost-effectiveness and normalized service delay, and then demonstrate the benefit of Wi-Fi solution quantitatively.

The main contributions of this paper are as follows:

- We deploy Wi-Fi APs at signalized intersections and study the fundamental influence of traffic signals on drive-thru Internet access, which has attracted significant research interest. Deploying AP at intersection can reduce the need for non-line-of-sight (NLOS) transmissions along the road so as to provide better service coverage [8]. One example of real-world deployment is *Wickedly Fast* Wi-Fi network which covers the downtown area of San Jose, CA, USA [9]. To facilitate the network performance analysis of urban drive-thru Wi-Fi networks, we develop a simple yet effective traffic modeling which to the best of our knowledge represents the first model to incorporate the influence of traffic lights at intersections on the throughput performance of a vehicle in a drive-thru Internet system. Interestingly, for the first time, we show a significant throughput gain for vehicles stopping at intersections due to red signals. Our modeling and analysis are validated via extensive SUMO and NS-3 simulations.
- We propose a framework for cost-effectiveness analysis of Wi-Fi network, in which the cost-effectiveness (how much TCO can be saved for the MNO) and normalized service delay (how much service degradation the vehicle user will tolerate) are mathematically defined and the explicit relation between these two metrics are established. Quantitatively, we show that the TCO of Wi-Fi can be traded with user's satisfaction, which could aid MNOs in strategic decision-making for Wi-Fi deployment. Our framework also lays a foundation for helping in understanding cost-effectiveness of other complementary wireless technologies for vehicle users, such as small cells in the context of cellular networks and super Wi-Fi operating in TV white space.

The remainder of the paper is organized as follows. Section II surveys the related works. Section III presents the problem formulation. We analyze the time-average throughput capacity of drive-thru Wi-Fi and the average downlink capacity of cellular network in Section IV and Section V, respectively. Section VI presents the cost-effectiveness analysis. Section VII provides concluding remarks.

II. RELATED WORK

A. Drive-thru Internet Access

There have been extensive research efforts on drive-thru Internet access. Due to high vehicle mobility and intermittent connectivity, network performance of drive-thru Wi-Fi is quite different from that of a normal Wi-Fi network. Many research efforts focus on performance evaluation through real-world measurement campaign in different scenarios, including urban area (e.g., [4]), highway (e.g., [5]), and traffic-free road (e.g., [10]). All these measurements show a limited throughput of per drive-thru access. To improve the performance of drive-thru Wi-Fi, a number of solutions have been proposed in the literature (refer to a survey [11] for details).

The first effort on analytical modeling of drive-thru Internet systems is presented in [12], which provides the closed-form expression of average number of bytes downloaded by a generic vehicle during its sojourn in an AP's coverage range considering both traffic flow theory and wireless network features. In this paper, we also propose an analytical model of drive-thru Internet access. Different from [12] only for uninterrupted traffic flows, we consider the fundamental influence of traffic signals, leading to an interrupted vehicle traffic. Moreover, our analysis is for the entire period during which vehicles travel through multiple Wi-Fi APs; whereas [12] focuses on the throughput of one typical drive-thru.

B. Cost-effectiveness Analysis

Research on cost-effectiveness of Wi-Fi solution for vehicular Internet access is quite limited. An apple-to-apple comparison of the performance characteristics of a 3G network and a metro-scale commercial Wi-Fi network (aiming to serve nomadic users) is performed in [13], and a hybrid network design is suggested to enhance the network performance. Fundamental relations between network throughput and infrastructure TCO are established in [14] for cellular deployment and Wi-Fi-based deployment, respectively. The Wi-Fi-based solution is suggested for providing a cost-effective data pipe to vehicles, however, without considering service delay/user's satisfaction and fundamental influence of traffic signals in urban scenarios. For vehicular ad hoc networks (VANETs), Banerjee *et al.* in [15] first examined the cost-performance tradeoffs for VANETs by considering three infrastructure enhancement alternatives: base stations (BSs), meshes, and relays. They demonstrated that if the average packet delay can be reduced by a factor of two by adding X BSs, the same reduction needs $2X$ meshes or $5X$ relays. They argued that relays or meshes can be a more cost-effective enhancement due to the high TCO of BSs. Note that the objective of their work is to improve network delay by augmenting mobile ad hoc networks with infrastructure, which is different from ours on cost-effectiveness of vehicular Internet access. Moreover, our methodology for modeling and analysis is also different from that adopted in [15]. Some other works (e.g., [16]) only consider cost issues of deploying a particular type of infrastructure.

III. PROBLEM FORMULATION

We study the cost-effectiveness of drive-thru Wi-Fi access in a city area Ω with a set of moving vehicles. Two different networking scenarios are considered. In the first scenario (Wi-Fi), the Internet gateways are sparsely deployed Wi-Fi APs (at intersections) and vehicles have only opportunistic drive-thru access. We use the second scenario (Cellular) with cellular macrocell BSs providing full service coverage as a benchmark for performance comparison.

We denote by N_W the number of Wi-Fi APs deployed in Wi-Fi scenario, and N_C the number of macrocell BSs deployed in Cellular scenario. In both scenarios, vehicles consume Internet data services as long as Internet connectivity is available. The maximum average data throughput achieved by individual vehicles are denoted by F_W and F_C , respectively for Wi-Fi and Cellular. To achieve a target aggregate throughput G (considering a mobile application of downloading a file of size G), the average time required (service delay) in Wi-Fi scenario and in Cellular scenario are denoted by D_W and D_C , respectively.

Definition 1: The normalized service delay (NSD) of a Wi-Fi deployment is defined as

$$\alpha = D_W/D_C.$$

Straightforwardly, the NSD characterizes the service quality degradation if the vehicle uses the Wi-Fi network instead of the cellular network. For a fixed deployment of cellular network (N_C), α merely depends on the deployment of Wi-Fi APs (N_W). From users' standpoint, a lower NSD is desirable, as the delay incurred to achieve a target throughput by using drive-thru Internet access would be easier to be tolerant instead of using fast but costly cellular services.

We denote by e_W the TCO (including CAPEX and OPEX) of deploying and operating one Wi-Fi AP. The total cost of a Wi-Fi deployment is thereby $\mathcal{E}_W = e_W N_W$. Similarly, we have e_C for deploying and operating one macrocell BS and $\mathcal{E}_C = e_C N_C$.

Definition 2: Cost-effectiveness of a Wi-Fi deployment is defined as

$$\eta = 1 - \mathcal{E}_W/\mathcal{E}_C \quad (1)$$

The cost-effectiveness is used to characterize the cost saving for deploying and operating a Wi-Fi infrastructure in a model city Ω . Intuitively, a lower NSD yields a lower cost-effectiveness. The NSD cannot be reduced while increasing the cost-effectiveness. The main objective of this paper is to study the tradeoff between α and η . A summary of the mathematical notations used in the paper is given in Table I.

IV. TIME-AVERAGE THROUGHPUT CAPACITY OF WI-FI

To obtain the service delay D_W , we first derive the time-average throughput capacity F_W of Wi-Fi network. In an urban environment, vehicle mobility is regulated by traffic signals at intersection, which imposes a significant impact on drive-thru Wi-Fi access: vehicle stopping at the intersection prolongs the connection time with the Wi-Fi AP so as to potentially increase the data volume downloaded/uploaded. To

TABLE I
THE KEY NOTATIONS.

Symbol	Description
Ω	Area of the target city
N_W	Number of Wi-Fi APs in the Wi-Fi scenario
N_C	Number of BSs in the Cellular scenario
F_W	Time-average throughput capacity of Wi-Fi
F_C	Time-average downlink capacity of Cellular
D_W	Average service delay of Wi-Fi
D_C	Average service delay of Cellular
G	Target aggregate throughput
α	Normalized service delay
e_W	Per infrastructure cost of Wi-Fi
e_C	Per infrastructure cost of cellular
\mathcal{E}_W	Total infrastructure cost of Wi-Fi
\mathcal{E}_C	Total infrastructure cost of Cellular
η	Cost-effectiveness of a Wi-Fi deployment
L	Distance between two adjacent intersections
R	Radius of Wi-Fi AP coverage
λ	Arrival rate of the vehicle flow to the AreaOI
τ	Length of traffic signal cycle
τ_g	Effective green period (EGP)
τ_r	Effective red period (ERP)
v	Constant vehicle speed unless it stops
Δ	Time loss due to vehicle acceleration
ρ	Density with which vehicles flow into the IArea
ρ_{max}	Jam density
$N(t)$	Number of vehicles in an AreaOI in a TSC
τ_a	Time instant when the tagged vehicle arrives at the IArea
$S(\tau_a)$	Sojourn time during which the tagged vehicle stays in an AreaOI
$\mu(t)$	Vehicle depart rate from the AreaOI, $t \in [0, \tau)$
$F(\tau_a)$	Throughput capacity per drive-thru achieved by the tagged vehicle
$\Upsilon(t)$	Maximum spectrum efficiency of cellular network (bits/s/Hz)

facilitate the throughput analysis, a simple yet effective modeling of vehicle flow regulated by traffic signals is developed.

A. Modeling Vehicle Flow with Fixed Signals

Appropriate modeling of vehicle flow regulated by traffic signals at intersections is the prerequisite to analyze the network performance of urban drive-thru Wi-Fi networks. However, it turns out to be a challenging task as it is difficult to determine how many details of vehicle mobility and road network should be incorporated into the modeling. Traffic models developed in transportation engineering, such as car following models, depend on many details/factors which increase the accuracy but could make the network analysis intractable or tedious. Hence, we develop a simple yet effective modeling with adequate details, which can capture the main characteristics of vehicle traffic at signalized intersections. To the best of our knowledge, our model represents the first model to incorporate the influence of traffic lights at intersections on the throughput performance of a vehicle in a drive-thru Internet system.

Road Network: The road network of the target city area Ω is considered as a regular grid, which is a common street pattern in many cities, such as Houston and Portland in U.S. [17]. In specific, we consider a two-way traffic on each road

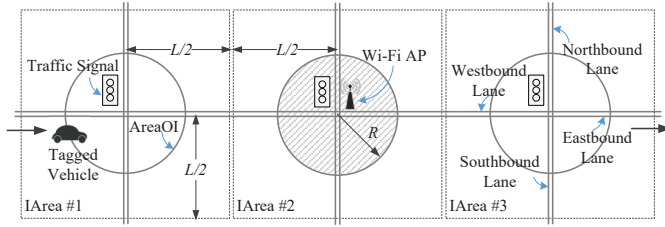


Fig. 1. Wi-Fi hotspot at signalized intersections.

and one single lane for each way. The intersection of any two roads is signalized, i.e., having traffic signal control. We denote by L the distance between any two neighboring intersections. Further, to facilitate our analysis, we define the intersection area (IArea) for each intersection. It is a square centering at one intersection and consisting four lanes (eastbound, westbound, northbound, and southbound) each of which is of length L , as shown in Fig. 1. By doing so, the city area is partitioned into distinct IAreas.

Wi-Fi Deployment: In Wi-Fi scenario, Wi-Fi APs are deployed in the target city area for vehicular Internet access. We consider the following random deployment strategy²: Wi-Fi APs are deployed only at intersections and an intersection has an AP deployed with probability p_{ap} . Deploying APs at intersections can reduce the need for non-line-of-sight (NLOS) transmissions along the road so as to provide better service coverage [8], which is also considered in literature, such as the theoretical study [7]. Moreover, placing APs at intersections mathematically facilitates the investigation on the impact of traffic signals due to the introduced symmetry. We denote by R the radius of AP coverage and define the area of interest (AreaOI) for each intersection, which is a disk centering at the intersection with radius R . The AreaOI thereby consists four lanes (eastbound, westbound, northbound, and southbound) each of which is of length $2R$, as shown in Fig. 1. It is obvious that if one intersection has an AP deployed, the AreaOI will be the Wi-Fi coverage region³.

Stop-and-Go Flow: The objective of this section is to analyze the throughput of drive-thru Wi-Fi network, considering the impact of road intersections controlled by traffic signals. To this end, we theoretically derive the vehicle connection time with AP (depending on the time the vehicle arrives at the intersection) and how many vehicles share the wireless resources within the AP coverage (changing over time during the connection period). Under the control of traffic signals, vehicles arriving at the intersection during the red period stop and form a queue, whereas vehicles arriving at the intersection during the green period keep going without delay if the vehicle queue is completely dissolved. In transportation engineering, many modeling approaches for signalized intersection focus on the development of delay and queue models [18]. The main

objective is to analyze the signal delay a vehicle experiences at the intersection (i.e., the extra waiting time due to signal operation and the vehicle queue), and the dynamics and the stochastic behavior of the overflow queue (i.e., the vehicle queue at the end of a green period). For example, one of the best-studied models is the fixed-cycle traffic light (FCTL) queue, where the traffic signal alternates between fixed green and red periods, and vehicles queued at the intersection are assumed to depart during the green period at equal time intervals [19]. However, the existing modeling approaches from traffic engineering cannot be directly applied to solve our problem. The reasons are two-fold: (i) the existing approaches focus on the steady-state or time-dependent analysis of delay and overflow queue length (the mean and the distribution), which are unable to characterize the dynamics of vehicle flow in the AreaOI; and (ii) the existing approaches are for the analysis of one-way traffic interrupted by traffic signals (the case of multiple lanes may be considered), and are too complex to apply to the scenario where the whole intersection area (including four lanes of different directions) is considered. In wireless networking research area, a stochastic traffic model is proposed for VANETs in signalized urban road systems [20], which can describe the average vehicle density and the random interactions among vehicles. The difficulty of applying this model to our scenario is also the high complexity. To describe the main behaviors of vehicle flow in the AreaOI, we have to ignore the minor details, such as the random behavior of individual vehicles. Thus, we develop a *stop-and-go* vehicle flow model controlled by fixed traffic signals. The proposed model is described as follows.

As a common practice, we simplify the three signal periods (i.e., green, amber, and red) into two periods, effective green period (EGP) and effective red period (ERP). We define the traffic signal cycle (TSC) $([0, \tau))$. For the eastbound and westbound lanes, an EGP $([0, \tau_g))$ is followed by an ERP $([\tau_g, \tau_g + \tau_r))$ during a TSC, whereas for the northbound and southbound lanes, an ERP $([0, \tau_g))$ is followed by an EGP $([\tau_g, \tau_g + \tau_r))$. The length of one TSC is hence denoted by $\tau = \tau_g + \tau_r$. We consider a deterministic vehicle flow, i.e., vehicles arrive at the IArea on each lane with arrival rate $\lambda(t) = \lambda$. Every vehicle keeps moving at the same and constant speed v unless it stops and joins a vehicle queue due to red signals. During the EGP⁴, each stopped vehicle departs the intersection at the speed v after a short delay Δ of being head-of-line. We introduce Δ to consider the time loss due to vehicle acceleration in reality. We also consider that vehicles do not change the lane at the intersection (i.e., no left, right, or U turns) for simplicity. Thus, vehicles flow into the IArea with a density ρ vehicle/m, and according to [21],

$$\rho = \lambda/v. \quad (2)$$

Further, we denote the jam density (maximum density) by ρ_{max} vehicle/m, which is the density of vehicles stopping and queuing at the intersection due to signal operations (typical range of ρ_{max} is 0.116 – 0.156 vehicle/m [22]).

⁴We make statement for the eastbound and westbound lanes unless otherwise specified.

²Although Wi-Fi APs may be regularly deployed at intersections, the encounter of next AP for a vehicle is still random due to the randomness in movement when we observe the vehicle. Therefore, we consider a random Wi-Fi deployment.

³We only consider the case in which $R < L/2$ so that there is no overlapped Wi-Fi coverage regions, which also makes economic sense.

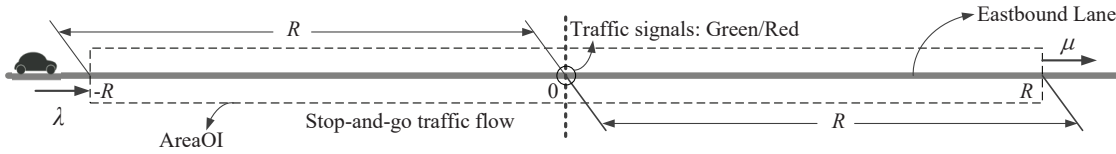


Fig. 2. Single-lane stop-and-go vehicle flow.

We analyze the performance of the urban drive-thru Wi-Fi network by observing a tagged vehicle. The tagged vehicle moves along a fixed lane (the eastbound lane in this study) and traverses IAreas in sequence, as shown in Fig. 1. To simplify our analysis, we have the following two assumptions⁵.

- *Unsaturation*: We consider the case that the length of vehicle queue is less than R , so that if the tagged vehicle stops at the intersection, it will always be in the AreaOI, i.e., the AreaOI is always unsaturated. In addition, we assume that there is no overflow queue, i.e., all queued vehicles can pass through the intersection during the EGP. This assumption is often valid under a regular traffic load condition and for a typical value of R .
- *Independence*: The IAreas are treated independently, i.e., traffic signals at different intersections are not coordinated and the vehicle arrival process for one IArea does not depend on the upstream traffic. We further assume that the tagged vehicle arrives at the IArea equally likely for any instant τ_a during the cycle $[0, \tau]$, i.e. τ_a is uniformly distributed over the interval $[0, \tau]$.

We denote by $N(t)$ the number of vehicles in an AreaOI in a TSC, where $t \in [0, \tau]$. Also, we denote by $S(\tau_a)$ the sojourn time the tagged vehicle stays in an AreaOI, where the arrival time $\tau_a \in [0, \tau]$. The sojourn time is equal to the connection time if there is an AP deployed in the intersection. Next, we derive the analytic expressions of $N(t)$ and $S(\tau_a)$.

B. Vehicle Dynamics

As shown in Fig. 2, we first focus on the vehicle flow regulated by traffic signals on the eastbound lane in a generic IArea, and denote the number of vehicles at time t in the AreaOI (only the eastbound lane is considered) by $N_e(t)$, where $t \in [0, \tau]$. We immediately have $N_e(0) = \lambda(\tau_r + R/v)$, which is the number of vehicles that arrive in the AreaOI but do not pass through the intersection during the previous TSC. Note that all these vehicles are located in $[-R, 0]$, i.e., $N_e(0)$ should be less than $\rho_{max}R$, according to the unsaturation assumption. Hence, vehicles arrive in the AreaOI at the rate $\lambda(t) = \lambda$ during $[0, \tau]$. As the arrival traffic would be regulated by the traffic signals, the vehicle departure rate from the AreaOI is the key to characterize $N_e(t)$. Let $\mu(t)$ denote this departure rate. $N_e(t)$ can be characterized as follows.

$$N_e(t) = N_e(0) + \int_0^t \lambda(\hat{t})d\hat{t} - \int_0^t \mu(\hat{t})d\hat{t}, \quad t \in [0, \tau]. \quad (3)$$

The departure rate function $\mu(t)$ is given by Lemma 1.

⁵Relaxation of these two assumptions would be considered for future works.

Lemma 1: Vehicles (on the eastbound lane) depart from the AreaOI at the rate $\mu(t)$, $t \in [0, \tau]$, where

$$\mu(t) = \begin{cases} 0, & t \in [0, \frac{R}{v} + \Delta); \\ \rho^*v, & t \in [\frac{R}{v} + \Delta, \frac{R}{v} + \Delta + t^*); \\ \lambda, & t \in [\frac{R}{v} + \Delta + t^*, \tau_g + \frac{R}{v}); \\ 0, & t \in [\tau_g + \frac{R}{v}, \tau), \end{cases}$$

where $\rho^* = \frac{\rho_{max}}{1 + \rho_{max}\Delta v}$ and $t^* = \frac{\lambda(\tau_r + \Delta)}{\rho^*v - \lambda}$.

Proof: Note that the time interval $[0, \tau_g)$ is the EGP and $[\tau_g, \tau)$ is the ERP. At $t = \Delta$, the head-of-line vehicle queued in the previous ERP starts to pass through the intersection at the speed v . Since the head-of-line vehicle has to move a distance of R to depart from the AreaOI, during $[0, \frac{R}{v} + \Delta)$, there is no vehicle departures. At $t = \frac{R}{v} + \Delta$, the vehicle queue with the density ρ^* starts to depart from the AreaOI, where ρ^* can be easily determined by the following equality: $\frac{1}{\rho_{max}} + \Delta v = \frac{1}{\rho^*}$. Next, we determine the duration of this departure, denoted by t^* . Since at $t = \frac{R}{v} + \Delta + t^*$, ρ^*vt^* vehicles have departed from the AreaOI and all the vehicles in the AreaOI are located in $[-R, R]$ with density ρ , we have the following equation with respect to t^* under the unsaturation assumption: $\lambda(\frac{R}{v} + \tau_r + \frac{R}{v} + \Delta + t^*) = \rho^*vt^* + \rho 2R$. From (2), we have $t^* = \frac{\lambda(\tau_r + \Delta)}{\rho^*v - \lambda}$. Therefore, during $[\frac{R}{v} + \Delta, \frac{R}{v} + \Delta + t^*)$, the departure rate is ρ^*v . Following the vehicle queue, vehicles depart at the arrival rate λ until $t = \tau_g + \frac{R}{v}$. Note that at $t = \tau_g$, the traffic signal turns from green to red. Again, there is no vehicle departure during $[\tau_g + \frac{R}{v}, \tau)$. ■

Thus, from (3) and Lemma 1, we have

$$N_e(t) = \begin{cases} \lambda(\tau_r + R/v + t), & t \in [0, \frac{R}{v} + \Delta); \\ \lambda(\tau_r + R/v + t) - \rho^*v(t - R/v - \Delta), & t \in [\frac{R}{v} + \Delta, \frac{R}{v} + \Delta + t^*); \\ 2\lambda R/v, & t \in [\frac{R}{v} + \Delta + t^*, \tau_g + \frac{R}{v}); \\ \lambda(R/v + t - \tau_g), & t \in [\tau_g + \frac{R}{v}, \tau). \end{cases} \quad (4)$$

Under the same control of traffic signals, the vehicle flow on the westbound lane has the same behavior as that on the eastbound lane. Thus, $N_w(t) = N_e(t)$, where $N_w(t)$ is the number of vehicles at time t on the westbound lane in the AreaOI. Similarly, $N_n(t)$ and $N_s(t)$ are denoted for the northbound and southbound lanes, respectively. $N_s(t) = N_n(t)$ and $N_n(t)$ can be derived in the same way as $N_e(t)$. The departure rate of vehicles on the northbound lane is given as follows: when $t \in [0, \frac{R}{v})$, $\mu(t) = \lambda$; when $t \in [\frac{R}{v}, \tau_g + \frac{R}{v} + \Delta)$, $\mu(t) = 0$; when $t \in [\tau_g + \frac{R}{v} + \Delta, \tau_g + \frac{R}{v} + \Delta + \frac{\lambda(\tau_r + \Delta)}{\rho^*v - \lambda})$, $\mu(t) = \rho^*v$; and when $t \in [\tau_g + \frac{R}{v} + \Delta + \frac{\lambda(\tau_r + \Delta)}{\rho^*v - \lambda}, \tau)$, $\mu(t) = \lambda$. Therefore,

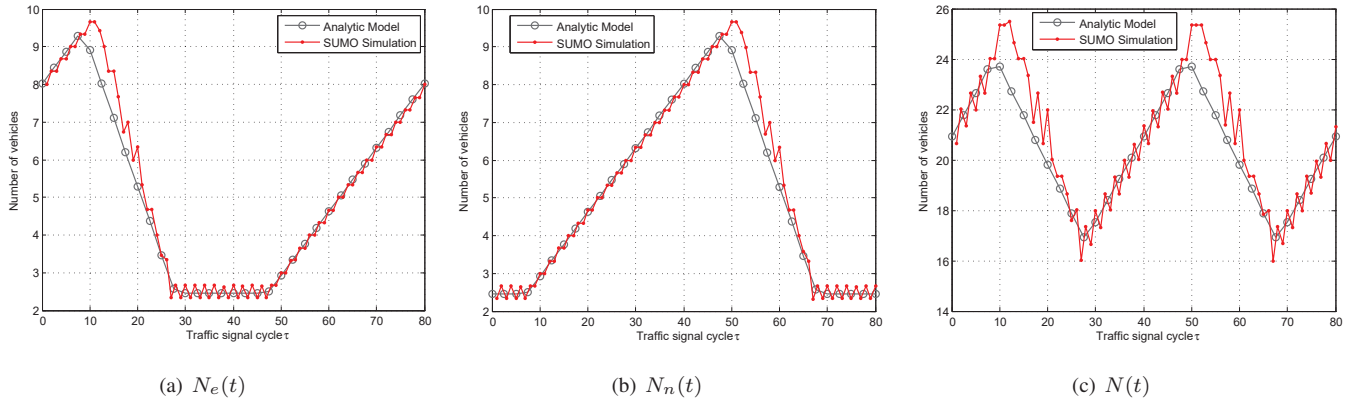


Fig. 3. Comparison of vehicle dynamics in the AreaOI between our analytic results and simulations based on SUMO. $\rho_{max} = 0.12$ vehicle/m, $v = 14$ m/s, $\lambda = 0.17$ vehicle/s, $\tau_r = \tau_g = 40$ s [23], $\Delta = 1.3$ s and $R = 100$ m.

we have

$$N_n(t) = \begin{cases} 2\lambda R/v, & t \in [0, \frac{R}{v}); \\ \lambda(R/v + t), & t \in [\frac{R}{v}, \tau_g + \frac{R}{v} + \Delta); \\ \lambda(R/v + t) - \rho^*v(t - \tau_g - R/v - \Delta), & t \in [\tau_g + \frac{R}{v} + \Delta, \tau_g + \frac{R}{v} + \Delta + \frac{\lambda(\tau_r + \Delta)}{\rho^*v - \lambda}); \\ 2\lambda R/v, & t \in [\tau_g + \frac{R}{v} + \Delta + \frac{\lambda(\tau_r + \Delta)}{\rho^*v - \lambda}, \tau). \end{cases} \quad (5)$$

As $N(t)$ is a summation of $N_e(t)$, $N_w(t)$, $N_n(t)$, and $N_s(t)$, we can immediately have the following result.

Lemma 2: Under the stop-and-go flow model and the unsaturation assumption, the number of vehicles in the AreaOI at time t , $t \in [0, \tau)$, is given by

$$N(t) = \begin{cases} 2\lambda(\tau_r + 3R/v + t), & t \in [0, \frac{R}{v}); \\ 2\lambda(\tau_r + 2R/v + 2t), & t \in [\frac{R}{v}, \frac{R}{v} + \Delta); \\ 2\lambda(\tau_r + 2R/v + 2t) - 2\rho^*v(t - R/v - \Delta), & t \in [\frac{R}{v} + \Delta, \frac{R}{v} + \Delta + t^*); \\ 2\lambda(3R/v + t), & t \in [\frac{R}{v} + \Delta + t^*, \tau_g + \frac{R}{v}); \\ 2\lambda(2R/v + 2t - \tau_g), & t \in [\tau_g + \frac{R}{v}, \tau_g + \frac{R}{v} + \Delta); \\ 2\lambda(2R/v + 2t - \tau_g) - 2\rho^*v(t - \tau_g - R/v - \Delta), & t \in [\tau_g + \frac{R}{v} + \Delta, \tau_g + \frac{R}{v} + \Delta + t^*); \\ 2\lambda(3R/v + t - \tau_g), & t \in [\tau_g + \frac{R}{v} + \Delta + t^*, \tau). \end{cases}$$

To evaluate how our proposed stop-and-go flow model can reflect the major behavior of vehicle dynamics in the AreaOI, we perform simulations in an open-source traffic software SUMO⁶ in which the car following model developed by Stefan Krauß [24] is used. We compare the obtained analytic results with simulation results, as shown in Fig. 3. The simulation data is averaged over 8,000 seconds (i.e., 100 traffic signal cycles). The fluctuation of simulation results is due to randomness of driver imperfection, which is a parameter controlled in the Stefan Krauß car following model, as shown in Table II.

C. Sojourn Time

The sojourn time $S(\tau_a)$ is the time duration the tagged vehicle stays in an AreaOI. Note that the sojourn time is

⁶SUMO is an open source, microscopic and continuous road traffic simulator designed to handle large road networks.

equal to the connection time for intersections with an AP deployed. $S(\tau_a)$ depends on the arrival time τ_a , which is uniformly distributed over the interval $[0, \tau)$. The analytic expression of $S(\tau_a)$ is given in the following lemma.

Lemma 3: Under the stop-and-go flow model and the unsaturation assumption, the sojourn time of the tagged vehicle given the arrival time τ_a is as follows.

$$S(\tau_a) = \begin{cases} \frac{\lambda(\tau_r + \frac{R}{v} + \tau_a)}{\rho^*v} + \frac{R}{v} + \Delta - \tau_a, & \tau_a \in [0, t^* + \Delta - \frac{R}{v}); \\ \frac{2R}{v}, & \tau_a \in [t^* + \Delta - \frac{R}{v}, \tau_g - \frac{R}{v}); \\ \frac{\lambda(\tau_a - \tau_g + \frac{R}{v})}{\rho^*v} + \frac{R}{v} + \Delta + \tau - \tau_a, & \tau_a \in [\tau_g - \frac{R}{v}, \tau). \end{cases}$$

Proof: Note that the tagged vehicle arrives in the location $-R$ at τ_a . It can be seen that the tagged vehicle will be the head of line in the vehicle queue if $\tau_a = \tau_g - \frac{R}{v}$. When $\tau_a \in [\tau'_a, \tau_g - \frac{R}{v})$, the tagged vehicle passes through the intersection without stop ($S(\tau_a) = 2R/v$), where τ'_a satisfies the following equality: $\lambda(\tau'_a + \tau_r + \frac{R}{v}) = \rho^*vt^*$. Hence, $\tau'_a = t^* + \Delta - \frac{R}{v}$. If $\tau_a \in [0, \tau'_a)$, the tagged vehicle will stop and join the vehicle queue because the vehicle queue formed during the previous ERP has not been dissolved yet. The sojourn time $S(\tau_a)$ is thereby $\frac{\lambda(\tau_r + \frac{R}{v} + \tau_a)}{\rho^*v} + \frac{R}{v} + \Delta - \tau_a$. When $\tau_a \in [\tau_g - \frac{R}{v}, \tau)$, the sojourn time of the tagged vehicle can be expressed as $\tau - \tau_a + \tau'_a$. The first part denotes the time elapsed before the traffic signal turning from red to green, and the second part denotes the time the tagged vehicle continues the movement until it departs from the AreaOI. τ'_a can be obtained by $\tau'_a = \frac{\lambda(\tau_a - \tau_g + \frac{R}{v})}{\rho^*v} + \frac{R}{v} + \Delta$. ■

D. Throughput Capacity Per Drive-thru

Based on Lemmas 2 and 3, we next derive the throughput capacity per drive-thru for the tagged vehicle.

Definition 3: Throughput capacity per drive-thru: the maximum number of bits received by the tagged vehicle from the Wi-Fi AP during one typical drive-thru of Wi-Fi coverage.

Wi-Fi transmission based on the IEEE 802.11 protocol adopts an adaptive modulation scheme with different transmission bit rates, depending on the communication distance

TABLE II
NS-3&SUMO SIMULATION PARAMETERS

SUMO Road Traffic				NS-3			
Parameter	Value	Parameter	Value	Parameter	Value	Parameter	Value
Acceleration	1.5 m/s ²	Deceleration	4.5 m/s ²	Wi-Fi standard	IEEE 802.11g	Rate Adaptation	AarWifiManager
Minimum vehicle gap	3 m	Maximum velocity	14 m/s	Physical layer model	YansWifiPhy	Channel model	YansWifiChannel
Vehicle's netto-length	5 m	Repetition period	6 s	Maximum transmission level	40 mW (≈ 130 m)	Data rate set	[1,2,5,5,6,9,11,12,18,24,36,48,54] mbps
Car-following model	SUMOKrauß	Driver imperfection	0.1	Propagation Loss	Log-Distance model	Path-loss exponent	4
Green (red) period	10~50 s	Amber period	1 s	Application model	OnOffApplication	Off-time period	0

TABLE III
STOP-AND-GO FLOW MODEL PARAMETERS FOR ANALYTIC RESULTS

Parameter	Value	Parameter	Value
λ	0.17 vehicle/s	v	14 m/s
ρ_{max}	0.12 vehicle/m	Δ	1.3 s
τ_r	10~50 s	τ_g	10~50 s
$\varphi_{max}C$	9 mbps	R	130 m

from the AP. However, to reduce the complexity of our model computation, we consider a non-adaptive scheme with constant transmission bit rate in a fixed AP coverage range. The non-adaptive transmission rate is also analytically considered in [12]. In addition, the contention-based MAC protocol, i.e., IEEE 802.11 DCF (distributed coordination function), is adopted to schedule parallel transmissions. To characterize the protocol overhead (including the overhead of physical layer), we introduce an empirical efficiency factor $\varphi \in (0, 1)$, which can be obtained from real-world measurements or through theoretical analysis. We consider that the tagged vehicle share the Wi-Fi resource equally with other vehicles in the AP's coverage range. Hence, the throughput capacity per drive-thru achieved by the tagged vehicle is given by

$$F(\tau_a) = \int_{\tau_a}^{\tau_a + S(\tau_a)} \frac{\varphi_{max}C}{N(t \bmod \tau)} dt, \quad (6)$$

where φ_{max} is the maximum efficiency factor for a given transmission rate and C is the AP's transmission rate. $\varphi_{max}C$ thereby indicates the maximum bit rate that can be utilized for data transmission. For example, according to [25], $\varphi_{max} = 5/11$ for IEEE 802.11b and $C = 11$ Mbps, as the theoretical maximum throughput is shown to be 5Mbps for a 11Mbps transmission rate. It is worthy noting that the throughput capacity per drive-thru depends on the arrival time of the tagged vehicle. That is to say with different arrival time to the AreaOI (with an AP deployed), the tagged vehicle achieves different throughput capacity per drive-thru, reflecting the impact of traffic signals. Particularly, there is a significant throughput gain for vehicles stopping at intersections due to red signals, as shown in the following simulation and analytic results, which is an important finding of this study.

To validate our modeling and analysis, we conduct simulations in the network simulator NS-3 and the road traffic simulator SUMO. We first use SUMO to generate the mobility trace file of vehicle traffic in one Area. And then, the trace file is used as an input for network simulations in NS-3. Simulation parameters and model parameters for analytic results are respectively given in Table II and Table III. Fig. 4

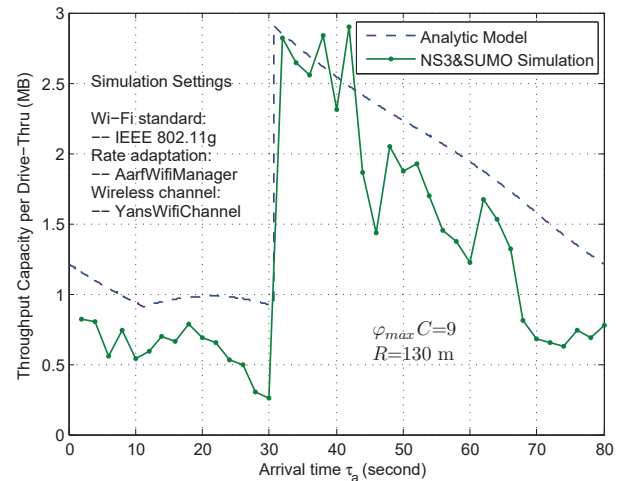


Fig. 4. $F(\tau_a)$ vs τ_a [$\tau_g = \tau_r = 40$ s].

presents the analytic and NS-3&SUMO simulation results on throughput capacity per drive-thru with respect to the arrival time. We adopt the IEEE 802.11g standard and adaptive data rates up to 54 Mbps in the simulation⁷. As the results shown in Fig. 4, vehicles arriving at the AreaOI with an arrival time around 31 seconds ($\tau_a \approx 31$) in a TSC, which thereby stop at the intersection due to the red signal so as to prolong the connection time with the AP, can achieve a much higher throughput capacity per drive-thru (approximately three times as high as the lowest one ($\tau_a \approx 11$) analytically), indicating a significant throughput gain. From Fig. 4, it can be seen that even with the none-adaptive data rate and simplified MAC operation, our theoretical and simulation measurements still match well in terms of general trends, which demonstrates

⁷We consider Wi-Fi standard IEEE 802.11g in the simulation evaluation for two reasons. Firstly, the IEEE 802.11g protocol is well developed in network simulator NS-3, which is widely recognized and used in academia. Secondly, employing other versions of Wi-Fi standard may yield slightly different results in the simulation. However, our result considering the IEEE 802.11g can be a benchmark once the performance bias of a different Wi-Fi standard over the IEEE 802.11g is known.

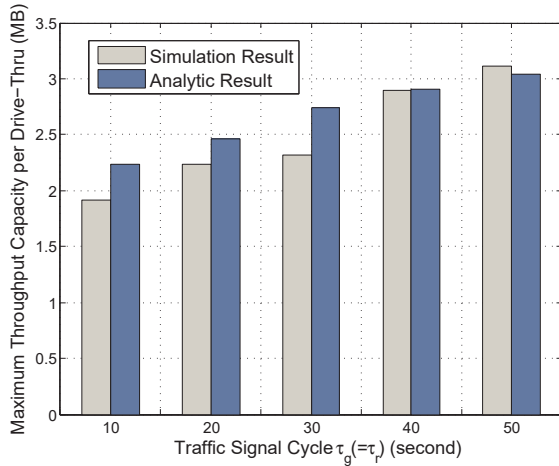


Fig. 5. $\max F(\tau_a)$, $\tau_a \in [0, \tau]$ vs τ_g .

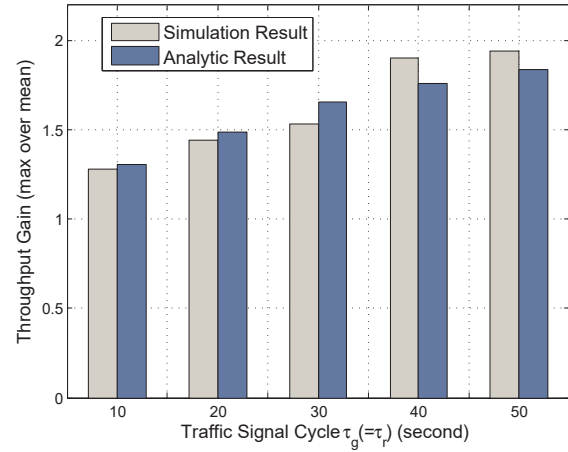


Fig. 6. Throughput gain (max over mean) vs τ_g .

the validity of our proposed modeling approach on throughput analysis of a vehicle driving through a Wi-Fi coverage considering the impact of traffic signals.

Fig. 5 presents the maximum throughput capacity per drive-thru, i.e., $F_{max} = \max_{\tau_a \in [0, \tau]} F(\tau_a)$, under different configurations of TSC. It is intuitive that with a longer EGP or ERP, vehicles achieve a larger F_{max} due to the prolonged connection time with the AP. However, the gain is not very significant since the increase of EGP or ERP also incurs a larger number of vehicles waiting at the intersection due to the red signal so as to increase the number of vehicles contending for Wi-Fi resources. As shown in Fig. 5, the impact of increasing the connection time after all dominates the impact of increasing the number of vehicles in the AP's coverage. Fig. 6 presents the throughput gain, which is the maximum value over the mean value of throughput capacity per drive-thru with respect to τ_a (mathematically defined as $\max_{\tau_a \in [0, \tau]} F(\tau_a) / [\frac{1}{\tau} \int_0^\tau F(\tau_a) d\tau_a]$), under different configurations of TSC. It can be seen that with a longer EGP or ERP, we have a higher throughput gain. For example, for $\tau_g = \tau_r = 40$ s, the maximum throughput capacity per drive-thru (achieved when $\tau_a \approx 31$ s) is 1.9 times the mean value by simulation and 1.8 times by analysis, demonstrating a significant impact of traffic signals.

E. Time-Average Throughput Capacity

The tagged vehicle moves along the road and experiences alternate disconnected period and connected period (being inside the AreaOI with an AP deployed). We are interested in the average bit rate of the tagged vehicle received from the APs over a long time, e.g., the entire travel time. Mathematically, we present the definition of time-average throughput capacity.

Definition 4: Time-average throughput capacity: the maximum average bit rate received by the tagged vehicle from the drive-thru Wi-Fi networks in a long term, which is given mathematically by

$$F_W = \lim_{t \rightarrow \infty} \frac{\tilde{F}(t)}{t}, \quad (7)$$

where $\tilde{F}(t)$ is the total number of bits received by time t .

We next derive the time-average throughput capacity. The Areas on the route of the tagged vehicle are indexed by $1, 2, \dots, n$, as shown in Fig. 1. Let T_n denote the time from the departure of the $(n-1)$ -th AreaOI to the departure of the n -th AreaOI. Thus, we have

$$T_n = (L - 2R)/v + S(\tau_a^n), \quad (8)$$

where τ_a^n is the arrival time to the n -th AreaOI. It can be seen that T_1, T_2, \dots, T_n are independent and identically distributed (i.i.d) random variables with a common distribution T under the independence assumption. Further, we denote by \tilde{F}_n the throughput capacity achieved in the n -th AreaOI. $\tilde{F}_n = F(\tau_a^n)$ with probability p_{ap} ; and $\tilde{F}_n = 0$ with probability $1 - p_{ap}$. The number of AreaOIs passed through by the tagged vehicle by time t is denoted by $\{I(t), t \geq 0\}$. Then, we have

$$\sum_{n=1}^{I(t)} \tilde{F}_n \leq \tilde{F}(t) < \sum_{n=1}^{I(t)+1} \tilde{F}_n. \quad (9)$$

Since \tilde{F}_n can be considered as the reward earned during the time period of T_n , we model $\{\tilde{F}(t); t > 0\}$ as a renewal reward process with inter-renewal time $\{T_n; n \geq 1\}$. The inter-renewal times have a finite expectation $E[T] < \infty$. $\tilde{F}_1, \tilde{F}_2, \dots, \tilde{F}_n$ are i.i.d random variables with a common distribution \tilde{F} . The following lemma holds for renewal reward processes.

Lemma 4: (Theorem 5.4.1 in [26]) Consider a renewal reward process $\{R(t); t > 0\}$ with expected inter-renewal time $E[X] = \bar{X} < \infty$. If each R_n is a random variable with $E[R_n] < \infty$, then with probability 1,

$$\lim_{t \rightarrow \infty} \frac{R(t)}{t} = \frac{E[R_n]}{\bar{X}}. \quad (10)$$

Proposition 1: Under the independence assumption, with probability 1, the time-average throughput capacity of the

tagged vehicle is given by

$$F_W = \frac{p_{ap} \int_0^\tau F(\tau_a) d\tau_a}{\tau(L - 2R)/v + \int_0^\tau S(\tau_a) d\tau_a}. \quad (11)$$

Proof: According to Lemma 4, $F_W = E[\tilde{F}]/E[T]$, as obviously we have $E[\tilde{F}] < \infty$ and $E[T] < \infty$. Specifically, from Lemma 3 and (8), $E[T] = \frac{L-2R}{v} + E[S(\tau_a)] = \frac{L-2R}{v} + \frac{1}{\tau} \int_0^\tau S(\tau_a) d\tau_a$. From (12), $E[\tilde{F}] = p_{ap} \frac{1}{\tau} \int_0^\tau F(\tau_a) d\tau_a$. Note that τ_a is uniformly distributed over $[0, \tau)$. We omit the tedious calculations of these two integrals. ■

It can be seen that the time-average throughput capacity of Wi-Fi network is determined by the urban environment (L), Wi-Fi deployment (p_{ap}), Wi-Fi coverage R , and connection time depending on traffic signal operation (τ_g, τ_r) and vehicle traffic (λ, v). The analytic and simulation results of F_W in terms of deployment scale are shown in Fig. 7. It can be seen that the time-average throughput capacity increases with a larger Wi-Fi deployment. Note that the analytic result is quite optimistic. This is because we use an empirical efficiency factor to simplify the MAC and physical layer operation of Wi-Fi. Our analytic result can be considered as an upper bound of Wi-Fi throughput performance.

V. BENCHMARK: CELLULAR MACROCELL SERVICE

The performance of cellular macrocell service is considered as a benchmark in the study of cost-effectiveness of Wi-Fi network. Thus, we use the networking scenario with cellular macrocell BSs providing full service coverage for performance comparison. A macrocell enables cellular services relying on a high-power cellular BS [27]. For apple-to-apple comparison, we assume that the considered cellular network only serves vehicle users. We focus on the analysis of average downlink capacity achieved by the tagged vehicle.

Definition 5: Average downlink capacity: the maximum average downlink data rate received from cellular BSs in a long term, which is given mathematically by

$$F_C = \lim_{t \rightarrow \infty} \frac{1}{t} \int_0^t U(t) dt, \quad (12)$$

where $U(t)$ is the instantaneous maximum data rate at time t .

A. Spectrum Efficiency

The maximum data rate $U(t)$ can be determined by $U(t) = b(t)\Upsilon(t)$, where $b(t)$ is acquired transmission bandwidth and $\Upsilon(t)$ is the maximum spectrum efficiency (bits/s/Hz), at time t . The maximum Spectrum efficiency is theoretically governed by the Shannon capacity. However, the Shannon capacity is not achievable in reality due to limited coding block length, non-avoidable system overhead, etc. [28]. Following [29], we adopt a modified Shannon capacity formula,

$$\Upsilon = \text{BW}_e \cdot \sigma \cdot \log_2 \left(1 + \frac{\text{SINR}}{\text{SINR}_e} \right), \quad (13)$$

where BW_e is the system bandwidth efficiency, SINR_e is the efficiency of signal-to-interference-plus-noise ratio (SINR),

and σ is a correction factor due to the dependency between SINR_e and SINR. Formula (13) can be used to approximate the maximum spectrum efficiency of real-world cellular systems with different settings. For example, for an LTE cellular system with single antenna transmissions and Round Robin scheduling, $\text{BW}_e \sigma = 0.56$ and $\text{SINR}_e = 2.0$ [29].

B. Distribution of SINR

The SINR on the wireless link between cellular BS and the tagged vehicle is an important basis to determine the downlink capacity. The interference experienced by the vehicle comes from the transmission of other-cell BSs. In urban areas with densely deployed BSs, other-cell interference is a major impediment to high spectrum efficiency [30]. To model the deployment of macrocell BSs in the considered area Ω , we consider a homogeneous Poisson point process (PPP) of density ξ , in which each point represents a location of BS. Modeling BS location as a PPP is widely adopted in the literature, e.g., [31] and [32], which is able to characterize the variety of macrocell size due to differences in transmission power, tower height, etc.. We consider the same vehicle density ρ as in the drive-thru Wi-Fi scenario. The impact of traffic signals on vehicle density is not considered here since cellular macrocell is much larger than Wi-Fi coverage and thereby not sensitive to such variations of vehicle density. Considering Rayleigh fading on other-cell interference, the complementary cumulative distribution function (CCDF) of SINR is given in [31], i.e.,

$$\Pr(\text{SINR} > Z) = \frac{1}{1 + Z^{\frac{2}{\beta}} \int_{Z^{-\frac{2}{\beta}}}^{\infty} \frac{1}{1 + u^{\beta/2}} du}, \quad (14)$$

where $\beta > 2$ is called the path-loss exponent. Typically, we have $\beta = 4$ for urban environments [33]. Thus, (14) can be further simplified as follows.

$$\Pr(\text{SINR} > Z) = \frac{1}{1 + \sqrt{Z}(\pi/2 - \arctan(1/\sqrt{Z}))} \quad (15)$$

The distribution of downlink SINR given in (15) is for the configuration of single transmit and single receive antenna. In addition, the thermal noise is ignored, as the urban cellular network is often interference-limited.

C. Average Downlink Capacity

To derive the average downlink capacity of the tagged vehicle, we consider a simple bandwidth sharing model: every vehicle can obtain a constant bandwidth b_0 from BSs, i.e., $b(t) = b_0$. Given that each BS provides a bandwidth of B , the total bandwidth resource in Ω is thus $\xi\Omega B$. As the total number of vehicles in Ω is given by $\Omega \cdot 4L\rho/L^2$ (approximately Ω contains Ω/L^2 iAreas and each iArea contains $4L\rho$ vehicles), we have $b_0 = \frac{\xi\Omega B}{4\rho}$. Considering the spectrum efficiency and distribution of SINR, the following result of average downlink capacity is obtained.

Proposition 2: The average downlink capacity of the tagged

vehicle is given by

$$F_C = \mathcal{U}_1 \int_{r>0} \frac{1}{1 + \sqrt{\mathcal{U}_2}(\pi/2 - \arctan(1/\sqrt{\mathcal{U}_2}))} dr, \quad (16)$$

where $\mathcal{U}_1 = \frac{\xi BLB\omega_e\sigma}{4\rho}$ and $\mathcal{U}_2 = \text{SINR}_e(2^r - 1)$.

Proof:

$$\begin{aligned} F_C &= \lim_{t \rightarrow \infty} \frac{1}{t} \int_0^t b(t)\Upsilon(t)dt = b_0 E[\Upsilon] \\ &= \frac{\xi BL}{4\rho} E \left[\text{BW}_e \sigma \log_2 \left(1 + \frac{\text{SINR}}{\text{SINR}_e} \right) \right] \\ &= \frac{\xi BLB\omega_e\sigma}{4\rho} \int_{r>0} \Pr \left(\log_2 \left(1 + \frac{\text{SINR}}{\text{SINR}_e} \right) > r \right) dr \\ &= \frac{\xi BLB\omega_e\sigma}{4\rho} \int_{r>0} \Pr \left(\text{SINR} > \text{SINR}_e(2^r - 1) \right) dr. \end{aligned}$$

The third equality holds due to $E[X] = \int_{x>0} \Pr(X > x)dx$ for a nonnegative random variable X . From (15), the proposition holds. ■

In the analysis of average downlink capacity, the inter-cell interference management techniques are not considered, such as frequency reuse. However, these advanced techniques are indeed beneficial for improving the spectrum efficiency and available data rates. Especially, the performance of LTE system is more limited by other-cell interference compared to 3G cellular systems [34], implying that interference management is also necessary for LTE systems. Hence, our result given in Proposition 2 is conservative and can be considered as a lower bound of average downlink capacity. In providing the benchmark cellular service for comparison, small cell service on top of the existing macrocell service is not considered. Under the same comparison level with Fig. 7, the analytic and simulation results of F_C in terms of deployment scale are shown in Fig. 8. It can be seen that the average downlink capacity increases with a larger cellular deployment in terms of ξ . We can also notice the conservativeness of our analytic result that we have discussed.

VI. COST-EFFECTIVENESS ANALYSIS

We examine the cost-effectiveness of Wi-Fi deployment in this section. For service delay of Wi-Fi scenario, mathematically, $D_W = E[\{\min t_0 : \tilde{F}(t_0) > G\}]$. Since it is difficult to obtain the distribution of $\tilde{F}(t)$ and given that $\Pr(\lim_{t \rightarrow \infty} \frac{\tilde{F}(t)}{t} = F_W) = 1$, D_W is approximated to be $\frac{G}{F_W}$ for a large G , e.g., one hundred MBytes. Similarly, $D_C \approx \frac{G}{F_C}$. Hence, the NSD $\alpha \approx F_C/F_W$.

The cost-effectiveness η depends on the TCO (including CAPEX and OPEX) of infrastructure node and the number of infrastructure node deployed in each scenario. The CAPEX includes the cost of equipment, planning, installation, commissioning, etc., and the OPEX includes the cost of site rental, power, maintenance, etc. [35]. Based on the cost model provided in [35], the ratio of the TCO of a Wi-Fi AP to the TCO of a macro 3-Sector LTE BS is around 12%, i.e., $e_W/e_C \approx 0.12$. To evaluate the cost-effectiveness of a Wi-Fi scenario, we fix the cellular deployment (Ω , N_C) and thereby the F_C is determined. Given that the average number of APs

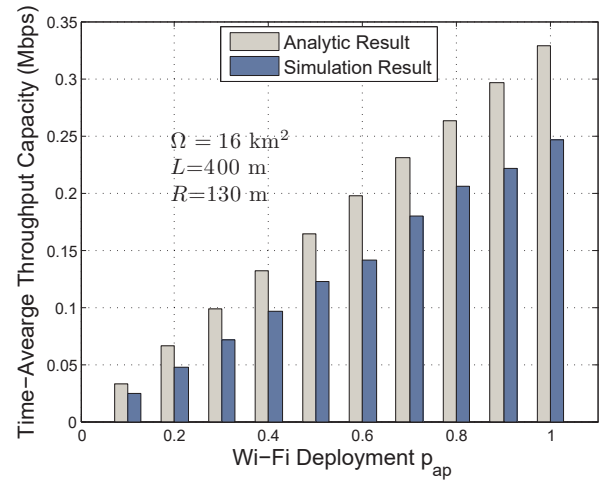


Fig. 7. F_W vs p_{ap} .

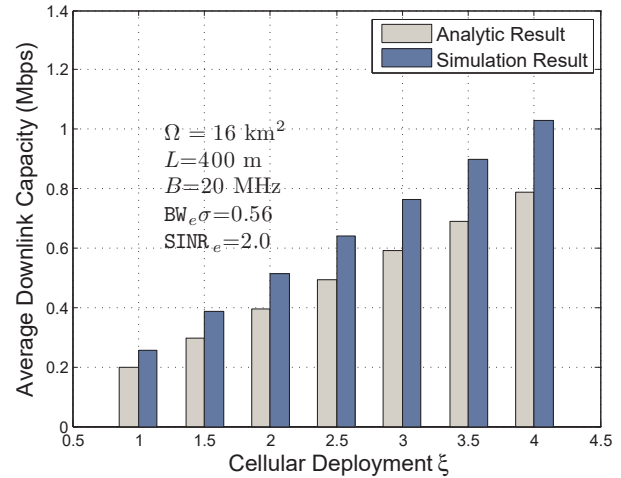


Fig. 8. F_C vs ξ .

deployed in a Wi-Fi scenario is $p_{ap}\Omega/L^2$, the explicit relation between η and α is given by

$$\eta = 1 - \frac{e_W}{e_C} \frac{\Omega F_C (\tau(L-2R)/v + \int_0^\tau S(\tau_a) d\tau_a)}{\alpha N_C L^2 \int_0^\tau F(\tau_a) d\tau_a}. \quad (17)$$

This is the main result of this paper, which presents the tradeoff between η (TCO savings) and α (service degradation). It can be seen that η depends on both controllable (e.g., Wi-Fi deployment (p_{ap} , R , α)) and uncontrollable (e.g., the urban environment (L , τ), vehicle traffic statistics (λ , v)) parameters. The analytic and simulation results on η are shown in Fig. 9. The gap between theory and simulation is due to the conservative result on F_C given in Proposition 2 (see Fig. 8). Through these results, the MNO is able to deploy Wi-Fi network according to the required level of service, and to have the knowledge of the corresponding TCO savings (compared to cellular solution) immediately. For example, theoretically from Fig. 9, almost 90% of the TCO can be saved if the average service delay of Wi-Fi deployment is 3X larger than that of cellular deployment, demonstrating the great potential of Wi-Fi solution for vehicle users in terms

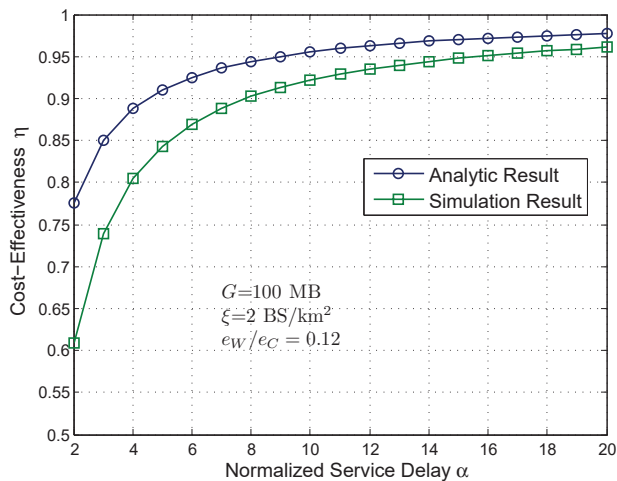


Fig. 9. Tradeoff between η and α [$\tau_r = \tau_g = 40$ s].

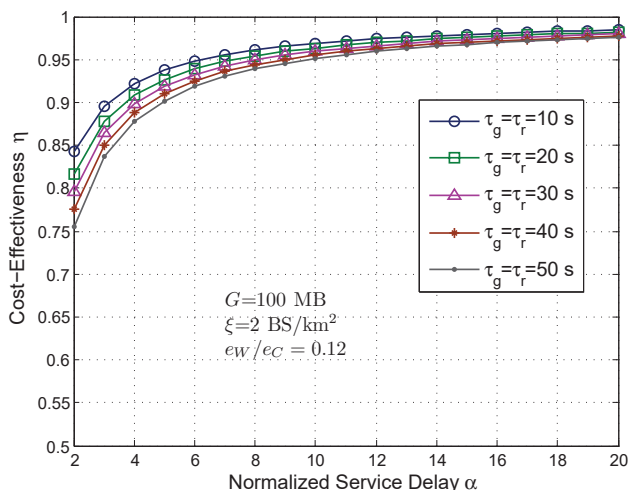


Fig. 10. Tradeoff between η and α under different configurations of TSC.

of cost-effectiveness. Fig. 10 analytically presents the tradeoff between η and α under different configurations of TSC. We can clearly see the impact of traffic signals on the tradeoff between the cost-effectiveness of Wi-Fi deployment and the service degradation. However, the impact is not significant especially for a large NSD. While for a single drive-thru, there exists a significant throughput gain due to the impact of traffic signals.

In our study, we do not consider deploying cellular macrocell BSs and Wi-Fi APs in one scenario for the purpose of apple-to-apple comparison and explicitly showing the great potential of Wi-Fi. For small cell cellular BSs (e.g., LTE small cells), although it is a promising solution to massive increase of mobile data demand, the feasibility of outdoor small cells for mobile user at vehicular speed is not clear yet. However, we believe that a heterogenous network with cellular macrocell service for coverage and cellular small cells and Wi-Fi for capacity would be desired. Also, in this paper, although we do not consider store-carry-and-forward communications between vehicles, which may incur additional cost/complexity for opportunistic data exchange, V2V communications can indeed

benefit Internet traffic delivery. For example, the vehicles in the coverage of Wi-Fi hotspots can help to relay the traffic so as to virtually extend the Wi-Fi service region.

VII. CONCLUSION

In this paper, we have investigated the cost-effectiveness of Wi-Fi solution for vehicular Internet access considering the tradeoff with the user's satisfaction. In Wi-Fi scenario, we have particularly studied the fundamental impact of traffic signals at intersection on Wi-Fi access. By examining the tradeoff between cost-effectiveness and normalized service delay, we have demonstrated that Wi-Fi has great potential to serve vehicle users with a much lower TCO. Our results provide a quick and efficient way of determining the Wi-Fi deployment strategy and the corresponding TCO savings. Future work includes large-scale simulations with real-world data set of vehicle mobility in urban scenarios, and cost-effectiveness analysis taking V2V communications into consideration.

REFERENCES

- [1] Transparency Market Research, *Connected Car Market -Global Industry Analysis, Size, Share, Growth, Trends and Forecast, 2013-2019*, 2013.
- [2] "OnStar LTE." [Online]. Available: <https://www.onstar.com/us/en/4glte/>
- [3] QUALCOMM, *Rising to Meet the 1000x Mobile Data Challenge*. Whitepaper, QUALCOMM Incorporated, San Diego, CA, USA, 2013.
- [4] V. Bychkovsky, B. Hull, A. Miu, H. Balakrishnan, and S. Madden, "A measurement study of vehicular internet access using in situ wi-fi networks," in *Proc. ACM MobiCom*, 2006.
- [5] J. Ott and D. Kutscher, "Drive-thru Internet: IEEE 802.11b for Automobile," in *Proc. IEEE INFOCOM*, Hong Kong, China, March 2004.
- [6] T. Wang, W. Jia, G. Xing, and M. Li, "Exploiting statistical mobility models for efficient Wi-Fi deployment," *IEEE Trans. on Vehicular Technology*, vol. 62, no. 1, pp. 360–373, 2013.
- [7] Z. Zheng, P. Sinha, and S. Kumar, "Sparse wifi deployment for vehicular internet access with bounded interconnection gap," *IEEE/ACM Trans. on Networking*, vol. 20, no. 3, pp. 956–969, 2012.
- [8] T. Mangel, M. Michl, O. Klemp, and H. Hartenstein, "Real-world measurements of non-line-of-sight reception quality for 5.9 GHz IEEE 802.11 p at intersections," in *Communication Technologies for Vehicles*. Springer, 2011, pp. 189–202.
- [9] "Wickedly Fast Wi-Fi." [Online]. Available: <http://www.wickedlyfastwifi.com/>
- [10] R. Gass, J. Scott, and C. Diot, "Measurements of in-motion 802.11 networking," in *Proc. IEEE Workshop on Mobile Computing Systems and Applications (WMCSA)*, Semiahmoo Resort, WA, USA, April 2005.
- [11] N. Cheng, N. Lu, N. Zhang, X. Shen, and J. W. Mark, "Vehicular wifi offloading: Challenges and solutions," *Vehicular Communications (Elsevier)*, vol. 1, no. 1, pp. 13–21, 2014.
- [12] W. L. Tan, W. C. Lau, O. Yue, and T. H. Hui, "Analytical models and performance evaluation of drive-thru internet systems," *IEEE JSAC*, vol. 29, no. 1, pp. 207–222, 2011.
- [13] P. Deshpande, X. Hou, and S. R. Das, "Performance comparison of 3G and metro-scale WiFi for vehicular network access," in *Proc. ACM SIGCOMM conference on Internet measurement*, Melbourne, Australia, November 2010.
- [14] N. Lu, N. Zhang, N. Cheng, X. Shen, J. W. Mark, and F. Bai, "Vehicles meet infrastructure: Towards capacity-cost tradeoffs for vehicular access networks," *IEEE Trans. on Intelligent Transportation Systems*, vol. 14, no. 3, pp. 1266–1277, 2013.
- [15] N. Banerjee, M. Corner, D. Towsley, and B. Levine, "Relays, base stations, and meshes: enhancing mobile networks with infrastructure," in *Proc. ACM MobiCom*, 2008.
- [16] H. Omar, W. Zhuang, and L. Li, "Gateway Placement and Packet Routing For Multihop In-Vehicle Internet Access," *IEEE Trans. on Emerging Topics in Computing*, to appear.
- [17] S. Kostof and R. Tobias, *The city shaped*. Thames and Hudson London, 1991.
- [18] F. Viti, *The dynamics and the uncertainty of delays at signals*. Netherlands TRAIL Research School, 2006.

- [19] J. S. van Leeuwen, "Delay analysis for the fixed-cycle traffic-light queue," *Transportation Science*, vol. 40, no. 2, pp. 189–199, 2006.
- [20] I. W.-H. Ho, K. K. Leung, and J. W. Polak, "Stochastic model and connectivity dynamics for VANETs in signalized road systems," *IEEE/ACM Trans. on Networking*, vol. 19, no. 1, pp. 195–208, 2011.
- [21] J. D. Fricker and R. K. Whitford, *Fundamentals of transportation engineering*. Pearson Prentice Hall, 2004.
- [22] M. Van Aerde and H. Rakha, "Multivariate calibration of single regime speed-flow-density relationships," in *Proc. the 6th Vehicle Navigation and Information Systems Conference*, 1995, pp. 334–341.
- [23] J. A. Bonneson, S. R. Sunkari, and M. P. Pratt, "Traffic Signal Operations Handbook," Texas Transportation Institute, Texas A & M University System, Tech. Rep., 2009.
- [24] S. Krauß, "Microscopic modeling of traffic flow: Investigation of collision free vehicle dynamics," Ph.D. dissertation, Universität zu Köln, 1998.
- [25] J. Jun, P. Peddabachagari, and M. Sichitiu, "Theoretical maximum throughput of IEEE 802.11 and its applications," in *IEEE International Symposium on Network Computing and Applications*, 2003.
- [26] R. G. Gallager, *Stochastic Processes: Theory for Applications*. Cambridge University Press, 2013.
- [27] J. H. Schiller, *Mobile communications*. Pearson Education, 2003.
- [28] E. Dahlman, S. Parkvall, J. Skold, and P. Beming, *3G evolution: HSPA and LTE for mobile broadband*. Academic press, 2010.
- [29] P. Mogensen, W. Na, I. Z. Kovács, F. Frederiksen, A. Pokhariyal, K. I. Pedersen, T. Kolding, K. Hugi, and M. Kuusela, "LTE capacity compared to the Shannon bound," in *Proc. IEEE VTC (Spring)*, 2007.
- [30] S. Mukherjee, "Distribution of downlink SINR in heterogeneous cellular networks," *IEEE JSAC*, vol. 30, no. 3, pp. 575–585, 2012.
- [31] J. G. Andrews, F. Baccelli, and R. K. Ganti, "A tractable approach to coverage and rate in cellular networks," *IEEE Trans. on Communications*, vol. 59, no. 11, pp. 3122–3134, 2011.
- [32] X. Lin, R. Ganti, P. Fleming, and J. Andrews, "Towards understanding the fundamentals of mobility in cellular networks," *IEEE Trans. on Wireless Communications*, vol. 12, no. 4, pp. 1686–1698, 2013.
- [33] H. Xia, "A simplified analytical model for predicting path loss in urban and suburban environments," *IEEE Trans. on Vehicular Technology*, vol. 46, no. 4, pp. 1040–1046, 1997.
- [34] D. Astély, E. Dahlman, A. Furuskar, Y. Jading, M. Lindstrom, and S. Parkvall, "LTE: the evolution of mobile broadband," *IEEE Communications Magazine*, vol. 47, no. 4, pp. 44–51, 2009.
- [35] M. Paolini and S. Fili, *The economics of small cells and Wi-Fi offload*. Report, SenzaFili Consulting, Sammamish, WA, USA, 2012.



Ning Zhang (S'12) earned the Ph.D. degree from University of Waterloo in 2015. He received his B.Sc. degree from Beijing Jiaotong University and the M.Sc. degree from Beijing University of Posts and Telecommunications, Beijing, China, in 2007 and 2010, respectively. His current research interests include smart grid, 5G, and vehicular networks.



and ICNC'15.

Ning Lu (S'12) received the B.Sc. (2007) and M.Sc. (2010) degrees from Tongji University, Shanghai, China, and Ph.D. degree from University of Waterloo, Waterloo, ON, Canada, all in electrical engineering. He is currently working as a postdoctoral fellow with the Department of Electrical and Computer Engineering at the University of Waterloo. His research focuses on fundamentals of wireless networking with special interest in connected vehicles. Mr. Lu served as a Technical Program Committee Member for IEEE PIMRC'12, WCSP'13, WCSP'14,



Nan Cheng (S'13) is currently a Ph.D. candidate in the department of Electrical and Computer Engineering, the University of Waterloo, Waterloo, ON, Canada. He received his B.S. degree and M.S. degree from Tongji University, China, in 2009 and 2012, respectively. Since 2012, he has been a research assistant in the Broadband Communication Research group in ECE Department, the University of Waterloo. His research interests include vehicular communication networks, cognitive radio networks, and resource allocation in smart grid.



Xuemin (Sherman) Shen (IEEE M'97-SM'02-F09) received the B.Sc.(1982) degree from Dalian Maritime University (China) and the M.Sc. (1987) and Ph.D. degrees (1990) from Rutgers University, New Jersey (USA), all in electrical engineering. He is a Professor and University Research Chair, Department of Electrical and Computer Engineering, University of Waterloo, Canada. He was the Associate Chair for Graduate Studies from 2004 to 2008. Dr. Shen's research focuses on resource management in interconnected wireless/wired networks, wireless

network security, social networks, smart grid, and vehicular ad hoc and sensor networks. He is an elected member of IEEE ComSoc Board of Governor, and the Chair of Distinguished Lecturers Selection Committee. Dr. Shen served as the Technical Program Committee Chair/Co-Chair for IEEE Infocom'14, IEEE VTC'10 Fall, the Symposia Chair for IEEE ICC'10, the Tutorial Chair for IEEE VTC'11 Spring and IEEE ICC'08, the Technical Program Committee Chair for IEEE Globecom'07, the General Co-Chair for ACM Mobihoc'15, Chinacom'07 and QShine'06, the Chair for IEEE Communications Society Technical Committee on Wireless Communications, and P2P Communications and Networking. He also serves/served as the Editor-in-Chief for IEEE Network, Peer-to-Peer Networking and Application, and IET Communications; a Founding Area Editor for IEEE Transactions on Wireless Communications; an Associate Editor for IEEE Transactions on Vehicular Technology, Computer Networks, and ACM/Wireless Networks, etc.; and the Guest Editor for IEEE JSAC, IEEE Wireless Communications, IEEE Communications Magazine, and ACM Mobile Networks and Applications, etc. Dr. Shen received the Excellent Graduate Supervision Award in 2006, and the Outstanding Performance Award in 2004, 2007, 2010, and 2014 from the University of Waterloo, the Premier's Research Excellence Award (PREA) in 2003 from the Province of Ontario, Canada, and the Distinguished Performance Award in 2002 and 2007 from the Faculty of Engineering, University of Waterloo. Dr. Shen is a registered Professional Engineer of Ontario, Canada, an IEEE Fellow, an Engineering Institute of Canada Fellow, a Canadian Academy of Engineering Fellow, and a Distinguished Lecturer of IEEE Vehicular Technology Society and Communications Society.



Jon W. Mark (M'62-SM'80-F'88-LF'03) received the Ph.D. degree in electrical engineering from McMaster University in 1970. In September 1970 he joined the Department of Electrical and Computer Engineering, University of Waterloo, Waterloo, Ontario, where he is currently a Distinguished Professor Emeritus. He served as the Department Chairman during the period July 1984-June 1990. In 1996 he established the Center for Wireless Communications (CWC) at the University of Waterloo and is currently serving as its founding Director. Dr. Mark had been

on sabbatical leave at the following places: IBM Thomas J. Watson Research Center, Yorktown Heights, NY, as a Visiting Research Scientist (1976-77); AT&T Bell Laboratories, Murray Hill, NJ, as a Resident Consultant (1982-83); Laboratoire MASI, Universit  Pierre et Marie Curie, Paris France, as an Invited Professor (1990-91); and Department of Electrical Engineering, National University of Singapore, as a Visiting Professor (1994-95). He has previously worked in the areas of adaptive equalization, image and video coding, spread spectrum communications, computer communication networks, ATM switch design and traffic management. His current research interests are in broadband wireless communications, resource and mobility management, and cross domain interworking.

Dr. Mark is a Life Fellow of IEEE and a Fellow of the Canadian Academy of Engineering. He is the recipient of the 2000 Canadian Award for Telecommunications Research and the 2000 Award of Merit of the Education Foundation of the Federation of Chinese Canadian Professionals. He was an editor of IEEE TRANSACTIONS ON COMMUNICATIONS (1983-1990), a member of the Inter-Society Steering Committee of the IEEE/ACM TRANSACTIONS ON NETWORKING (1992-2003), a member of the IEEE Communications Society Awards Committee (1995-1998), an editor of Wireless Networks (1993-2004), and an associate editor of Telecommunication Systems (1994-2004).



Fan Bai (General Motors Global R&D) is a Senior Researcher in the Electrical & Control Integration Lab., Research & Development and Planning, General Motors Corporation, since Sep., 2005. Before joining General Motors research lab, he received the B.S. degree in automation engineering from Tsinghua University, Beijing, China, in 1999, and the M.S.E.E. and Ph.D. degrees in electrical engineering, from University of Southern California, Los Angeles, in 2005.

His current research is focused on the discovery of fundamental principles and the analysis and design of protocols/systems for next-generation Vehicular Ad hoc Networks (VANET), for safety, telematics and infotainment applications. Dr. Bai has published about 40 book chapters, conference and journal papers, including Mobicom, INFOCOM, MobiHoc, SECON, ICC, Globecom, WCNC, JSAC, IEEE Wireless Communication Magazine, IEEE Communication Magazine and Elsevier AdHoc Networks Journal. In 2006, he received Charles L. McCuen Special Achievement Award from General Motors Corporation in recognition of extraordinary accomplishment in area of vehicle-to-vehicle communications for drive assistance & safety. He serves as Technical Program Co-Chairs for IEEE WiVec 2007 and IEEE MoVeNet 2008. He is an associate editor of IEEE Transaction on Vehicular Technology and IEEE Transaction on Mobile Computing, and serves as guest editors for IEEE Wireless Communication Magazine, IEEE Vehicular Technology Magazine and Elsevier AdHoc Networks Journal. He is also serving as a Ph.D. supervisory committee member at Carnegie Mellon University and University of Illinois-Urbana Champaign.